

Physically-based Two-stage Underwater Image Restoration

Nan Wang¹, Lin Qi¹, Junyu Dong^{1*}, Hao Fan¹, Xingnan Chen¹, Hui Yu²

¹Ocean University of China ²University of Portsmouth
dongjunyu@ouc.edu.cn

ABSTRACT

Underwater images are blurred due to light scattering and absorption. Image restoration is therefore important in many underwater research and practical tasks. In this paper, we propose an effective two-stage method to restore underwater scene images. Based on an underwater light propagation model, we first remove backscatter by fitting a binary quadratic function. Then we eliminate the forward scattering and non-uniform lighting attenuation using blue-green dark channel prior. The proposed method requires no additional calibration and we show its effectiveness and robustness by restoring images captured under various underwater scenes.

Keywords: Underwater image restoration; backscatter removal; dark channel prior; underwater lighting propagation model.

1. INTRODUCTION

Light propagation in the water is heavily attenuated due to the absorption and scattering by numerous suspending particles. Underwater images are accordingly blurred. Restoration of underwater images is therefore important for oceanographic exploration and computer vision tasks such as underwater 3D reconstruction. The key to underwater image restoration is to remove the influence of absorption and scattering. In addition to studying light transmission in the water [1, 2, 3, 4], researchers also made efforts in investigating how light propagates in different medium environment, like hazy and foggy scenes [5, 6, 7].

A challenging problem of underwater image restoration is backscatter removal. Some work proceeds with directly estimating the parameters in traditional optical propagation model [1, 4]. And other approaches indirectly solve the complex problem with the assist of polarization [8, 9] or fitting some specific function like the binary quadratic function [3], achieving good result as well.

Traditional dehazing techniques have been applied in underwater scenes as their propagation models share some similarities. Dark channel prior [7], which has been widely researched in many fields, was also found to be able to improve the quality of underwater images [10].

Different methods mentioned above appear with distinctive features, but also limitations exist. The estimation of complex optical propagation parameters calls for specific scenes assumption and necessary approximation, which brings strict limit with complicated calculation. Dark channel prior method has a certain effect in underwater images processing [10], but the underwater propagation model is different from the dehazing model, which contains dominant component of backscatter.

In this paper, we propose a novel two-stage approach to restore underwater images without additional pre-requisite calibration. First, we improve the backscatter removal method in [3] by separating the background pixels from the image, from which we use a more reasonable function fitting method to estimate the backscatter. Second, we propose a new model with blue-green dark channel prior to remove the forward scattering and spatially dependent absorption. An example of our restoration result is shown in Figure 1.

Our first contribution is that we improve the method for robustly removing global backscatter. We use RANSAC to fit the binary quadratic function from the separated background without any calibration. The second contribution is that we present a more accurate underwater propagation model with blue-green dark channel method.

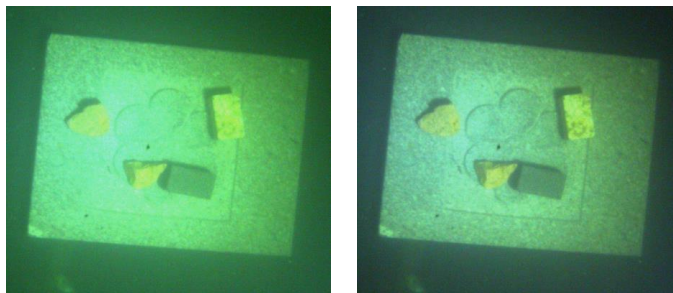


Figure 1. The original image captured in underwater environment (left) and the restoration result (right).

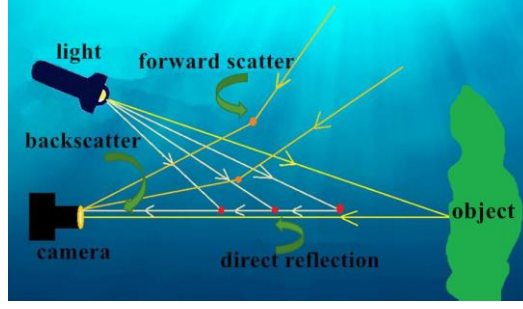


Figure 2. Underwater light propagation model. The intensity of the image is the sum of direct reflection, backscatter and forward scatter.

2. IMAGE FORMATION MODEL

In this section, we introduce the underwater image formation model. We assume the object surface is Lambertian with uniform albedo. As Figure 2 shows, the object is imaged on the image plane. Each point $\mathbf{X} = (X, Y, Z)$ on the object surface in world's coordinate maps to the corresponding point $\mathbf{x} = (x, y)$ in image coordinate. When multiple light sources exist, the intensity of point \mathbf{X} illuminated by source k on the image is $I^k(\mathbf{x})$. In a single scattering medium, $I^k(\mathbf{x})$ can be separated into three parts:

$$I^k(\mathbf{x}) = D^k(\mathbf{x}) + B^k(\mathbf{x}) + F^k(\mathbf{x}) \quad (1)$$

where $D^k(\mathbf{x})$ is the directly reflected light from the object surface, $B^k(\mathbf{x})$ is the backscatter which is the sum of light reflected from numerous suspending particles in the medium, and $F^k(\mathbf{x})$ is the forward scattering from ambient light.

In a turbid medium, light is attenuated exponentially with distance. Suppose the radiance of light reflected from the point \mathbf{X} is $R^k(\mathbf{X})$, then we can rewrite the direct reflection as:

$$D^k(\mathbf{x}) = R^k(\mathbf{X})e^{-\sigma d(\mathbf{x})} \quad (2)$$

where σ is the distinction coefficient and $d(\mathbf{x})$ represents the distance between \mathbf{X} and \mathbf{x} . Our aim is to restore $R^k(\mathbf{X})$ given the input image $I^k(\mathbf{x})$. In the following two sections we introduce our proposed two-stage method to remove the backscatter part and finally restore $R^k(\mathbf{X})$.

3. STAGE ONE: BACKSCATTER REMOVAL

Removing scattering component from a single image is an intractable problem. When a light source is placed on the same side of the camera, which is the normal setting of most underwater image systems, the total backscattered light reaching to the camera is the sum of all backscatter components along the reflection axis. Tsitsios et al. [3] proposed to estimate backscatter from the darkest pixel in a local region of dark background. The distribution of global backscatter was approximated using a binary quadratic function based on the assumption of point light source. Their strict experimental setting requires pre-calibration of the dark scene for accurate backscatter fitting, and the restoration result can be degraded without calibration when the local regions containing object are misclassified as background.

In this paper, we modified the method above to estimate the backscatter without calibrating in advance. For an input single image containing dark background and target object, our backscatter removal method takes following steps:

(1) Bilateral filtering. To suppress the low frequency noise and preserve details, we use a high-pass bilateral filter to preprocess the input image.

(2) Background extraction. We separate the background from the image using graph-based segmentation. To filter out the object regions, we reset the object regions with brighter RGB intensity (set to be 255) to avoid later process.

(3) Block filtering. We divide the image into blocks (8×8 pixels in our experiment). The regions with lower intensity are more likely to represent the backscatter, so we first filter out the overall brighter regions. We calculate the sum of intensities in each block as $sum_{i,j}^k$, where k represents the channel of red, green or blue and i, j indicates the block location. We discard the blocks whose $sum_{i,j}^k$ is larger than a threshold γ . The optimum threshold is related to the size of the blocks, and a smaller threshold is called when we set the size smaller. The location and intensity of the darkest point in each block are recorded for the next step.

(4) Function fitting with RANSAC. We can estimate a binary quadratic function with at least six points. In the first round, the optimal function is recorded with the maximum inliers. Then we carry out the second round using all the inliers of the optimal function in the first round. The optimal scheme in the second round is recorded as the final result.

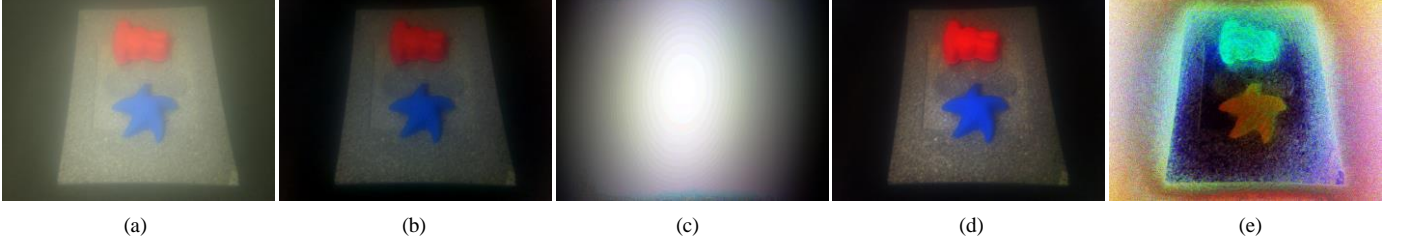


Figure 3. Our restoration result in different stages. (a) Input image. (b) The result after using our backscatter removal method. (c) Difference between (a) and (b) with additional histogram equalization process for better visualization. (d) Final restoration image. (e) Difference between (b) and (d) with histogram equalization.

(5) Backscatter removal. We use the function estimated in the previous step to calculate the backscatter of each point and remove it by a simple subtraction from the image.

Using the method above, we can eliminate the dominant noise in underwater images. In the next section $R^k(\mathbf{X})$ is finally restored based on a modified dehazing model.

4. STAGE TWO: FINAL RESTORATION

Figure 3(b) shows the improvement after removing backscatter using the method above. However, for applications that require high details such as photometric stereo, forward scatter and the effect of non-uniform attenuation needs to be removed. Dark channel prior method has shown its success in dehazing, and has been applied in underwater image processing [10]. However, the underwater lighting model is different from the dehazing model, especially when artificial light source is added. In foggy environment, the dominant component of the light is the ambient light. On the contrary, the backscatter takes dominant proportion in the underwater scene, based on which we transferred the modified dark channel prior on the second stage.

Defining the intensity of \mathbf{x} after backscatter removal as $I_{-B}^k(\mathbf{x})$, we rewrite the light formation model as:

$$I_{-B}^k(\mathbf{x}) = D^k(\mathbf{x}) + F^k(\mathbf{x}) = J^k(\mathbf{x}) t^k(\mathbf{x}) + A^k \alpha (1 - t^k(\mathbf{x})) \quad (3)$$

where $J^k(\mathbf{x})$ is the light intensity of channel k reflecting from the object surface (imaging on the point \mathbf{x}), which is the part we aim to restore; A^k is the ambient light of channel k ; $t^k(\mathbf{x})$ represents the medium transmission, which can be written as $t^k(\mathbf{x}) = e^{-\sigma^k d(\mathbf{x})}$, also named as attenuation rate; α is a coefficient calculated by the ratio between forward scatter part and all attenuation part (absorption, backscatter and forward scatter), which is not considered in traditional dehazing model.

Unlike in the atmosphere, the attenuation is obvious in underwater environment and varies significantly with wavelength. The light in red channel suffers serious optical attenuation, so we only define the blue-green dark channel as:

$$J^{dark}(\mathbf{x}) = \min_{y \in \Omega(\mathbf{x})} (\min_{k \in \{G, B\}} J^k(y)) \quad (4)$$

where $\Omega(\mathbf{x})$ is a small patch around point \mathbf{x} . He et al. [7] showed that some pixels usually have very low intensity in at least one color (RGB) channel in most haze free regions. We find it also applicable to underwater images. For the blue-green dark channel image, the intensity $J^{dark}(\mathbf{x})$ can be described as the extent of the opacity, and the regions with local high intensity will be considered as the opaque regions. When artificial source exists, multiple scattering makes up the strong ambient light intensity A^k , which is bigger than $J^k(\mathbf{x})$ along a single optical path. As the transmission of opaque regions is close to zero, A^k can be estimated as:

$$A^k = \frac{I^k(\mathbf{x}) - \min_{y \in \Omega(\mathbf{x})} (\min_{k \in \{G, B\}} J^k(y)) t^k(\mathbf{x})}{\alpha (1 - t^k(\mathbf{x}))} \approx \frac{I^k(\mathbf{x})}{\alpha} \quad (5)$$

We take top 0.1% brightest points in the dark channel, which are considered as opaque regions, then calculate the average of these points in the image for each channel as $I_{average}^k(\mathbf{x})$. The ambient light A^k can be described as $\frac{I_{average}^k(\mathbf{x})}{\alpha}$. As the specific value of α is unknown, we can only obtain the value of αA^k .

The next step is to estimate the distribution of $t^k(\mathbf{x})$. We can extract $t^k(\mathbf{x})$ from equation (3):

$$t^k(\mathbf{x}) = \frac{I_{-B}^k(\mathbf{x}) - \alpha A^k}{J^k(\mathbf{x}) - \alpha A^k} \quad (6)$$

We assume that the transmission rate in each patch is equal, which is denoted as $\tilde{t}(\mathbf{x})$. Equation (6) can then be rewritten with blue-green dark channel:

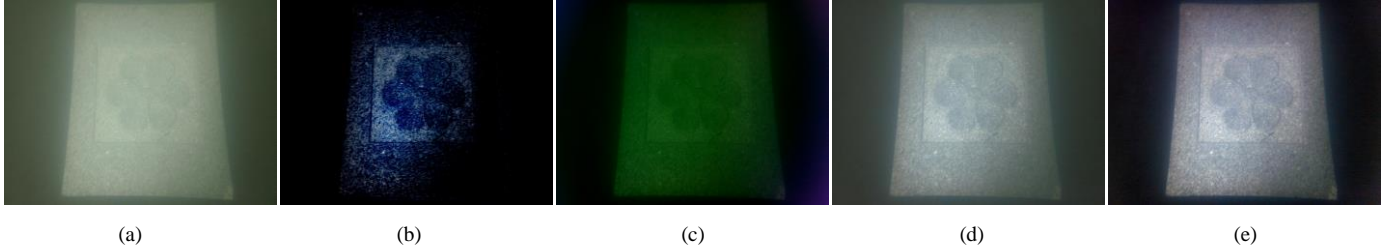


Figure 4. Comparison with other methods. (a) Input image. (b) Fattal's result [6]. (c) Result of unimproved backscatter removal method [3]. (d) Result of directly using dark channel prior [10]. (e) Our result.

$$\tilde{t}(\mathbf{x}) = \frac{\min_{y \in \Omega(\mathbf{x})} \left(\min_{k \in \{G, B\}} I_B^k(y) \right) - \alpha A^k}{\min_{y \in \Omega(\mathbf{x})} \left(\min_{k \in \{G, B\}} J^k(y) \right) - \alpha A^k} \quad (7)$$

Since J with three channels is the aim image with no attenuation, the blue-green dark channel of J is close to zero due to dark channel prior. So $\tilde{t}(\mathbf{x})$ can be simplified as:

$$\tilde{t}(\mathbf{x}) = 1 - \frac{\min_{y \in \Omega(\mathbf{x})} \left(\min_{k \in \{G, B\}} I_B^k(y) \right)}{\alpha A^k} \quad (8)$$

We can roughly estimate the coarse transmission distribution of each patch by equation (8). However, the transmission map has mosaic effects. To optimize the transmission result, we process the transmission image using guided filter [11].

In the last step, $J^k(\mathbf{x})$ is restored with the equation derived from equation (3):

$$J^k(\mathbf{x}) = \frac{I^k(\mathbf{x}) - \alpha A^k}{\max(t_m, \tilde{t}(\mathbf{x}))} + \alpha A^k \quad (9)$$

where t_m is the threshold of transmission estimation in case the estimated transmission rate is too small (0.2 in our experiment). Please note that the value of α has no effect on the final estimation.

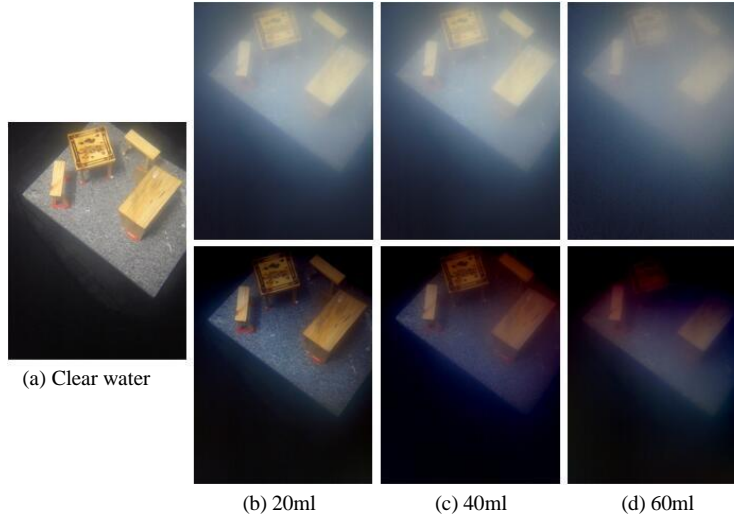


Figure 5. The restoration result of different turbidity. (a) The image captured in clear water. (b)(c)(d) are the input images and the corresponding restoration result when different amount of milk is added. The first line of images are the input and the second line with restoration result.

5. EXPERIMENTAL RESULTS

Our experimental setup consists of a glass tank of the size 1m×1m×1m. The inner wall of the tank is wrapped with black canvas to simulate the dark background. The camera and artificial light source are fixed on a steel frame placed upon the tank, both of which are immersed in the water with waterproof covers. In our experiment, we add milk to simulate the underwater turbidity.

The result of our image restoration is shown in Figure 3. Figure 3(c) and Figure 3(e) show the changes of the two stages. We can see from Figure 3(c) that the first stage of backscatter removal reflects a global change, unrelated to the object. In contrast, Figure 3(e) shows the change in object details during the second stage of image process.

In Figure 4 we compare our method with some classical methods in the literature. Fattal’s method [6] is based on the local variance and requires color information, which is not suitable for underwater images. Figure 4(c) shows the result of unimproved backscatter removal method [3]. As we mentioned before, this method is not robust without previous calibration of the scene, which may misuse object regions to fit the binary quadratic function. Figure 4(d) shows the result of directly using dark channel prior to process the input image. The result shows improvement in details, but it is also obviously that the blurring effect in global regions has not been removed, which just corresponds to the backscatter. To analyze the robustness of our method, we constructed more complex scenes of different turbidity by adding different quantities of milk to the water. The restoration comparison is shown in Figure 5.

Table 1. PSNR comparison of Figure 4.

Method	PSNR
Fattal [6]	15.764
Tsiotsios et al. [3]	14.782
Carlevaris-Bianco et al. [10]	18.826
Our method	24.253

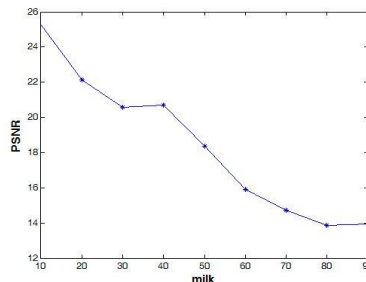


Figure 6. PSNR of the restoration result with different turbidity.

We further evaluate the quality of the restoration result in terms of peak signal-to-noise ratio (PSNR), which can reflect the similarity between the two images. In our experiment we used the image captured in clear water as the standard image, and compared restoration result with it. The higher value of PSNR indicates more similarities. Table 1 shows PSNR of the results in Figure 4, from which we can see our method outperforms other methods with the highest PSNR. Figure 6 presents the detailed analysis of Figure 5. The restoration result is going worse as the turbidity increases, and when 80 ml milk is added, we can hardly identify the details in the restored images.

6. CONCLUSION AND FUTURE WORK

In this paper we proposed an effective two-stage method of underwater image restoration. To remove the backscatter, we improved the method by fitting backscatter using RANSAC. We then used an optimized blue-green dark channel prior method to remove forward scatter and the impact of non-uniform attenuation rate distribution. We demonstrated the superiority of our method over previous methods with experiments in complex underwater scenes.

Our method also has its limitation. The image restoration method with single input image requires some regions of dark background for accurate fitting. The method cannot work well in extremely non-uniform lighting conditions.

For future work, more complex functions can be considered to approximate the backscatter distribution instead of the simple binary quadratic function, especially for complex lighting scenes. The restored images can be used in subsequent high level applications such as underwater 3D reconstruction to verify the effectiveness of our method.

REFERENCES

- [1] S. G. Narasimhan, S. K. Nayar, B. Sun, and S. J. Koppal. Structured Light in Scattering Media. In Computer Vision, 2005. ICCV 2005. Tenth IEEE International Conference on, volume 1, pages 420-427, 2005.
- [2] Y. Y. Schechner and N. Karpel. Clear underwater vision. Computer Vision and Pattern Recognition, 2004. CVPR 2004. Proceedings of the 2004 IEEE Computer Society Conference on, volume 1, pages I-536-I-543, 2004.
- [3] C. Tsiotsios, M. E. Angelopoulou, T.-K. Kim, and A. J. Davison. Backscatter compensated photometric stereo with 3 sources. In Computer Computer Vision and Pattern Recognition (CVPR), 2014 IEEE Conference on, 2259-2266.
- [4] Z. Murez, T. Treibitz, R. Ramamoorthi, and D. Kriegman. Photometric Stereo in a Scattering Medium. In IEEE International Conference on Computer Vision (ICCV), pages 3415-3423, 2015.
- [5] R. T. Tan. Visibility in bad weather from a single image. Computer Vision and Pattern Recognition, 2008. CVPR 2008. IEEE Conference on, pages 1-8, 2008.
- [6] R. Fattal. Single Image Dehazing. ACM transactions on graphics (TOG), 2008.
- [7] K. He, J. Sun, and X. Tang. Single image haze removal using dark channel prior. IEEE Transactions on Pattern Analysis and Machine Intelligence, volume 33, issue 12, pages 2341-2353, 2010.
- [8] G. D. Lewis, D. L. Jordan, and P. J. Roberts. Backscatter target detection in a turbid medium by polarization discrimination. App. Opt., 38:3937-3944, 1999.
- [9] T. Treibitz and Y. Y. Schechner. Active Polarization Descattering. IEEE Transactions on Pattern Analysis and Machine Intelligence, volume 31, Issue 3, pages 385-399, 2009.
- [10] N. Carlevaris-Bianco, A. Mohan, and R. M. Eustice. Initial results in underwater single image dehazing. In Proc. of IEEE OCEANS 2010, pages 1-8 (2010).
- [11] K. He, J. Sun, and X. Tang. Guided Image Filtering. IEEE Transactions on Pattern Analysis and Machine Intelligence, volume 35, issue 6, pages 1397-1409, 2013.

AUTHORS' BACKGROUND

Your Name	Title*	Research Field	Personal Website
Nan Wang	master student	Image processing, 3D reconstruction	
Lin Qi	associate professor	Computer vision, 3D reconstruction	https://www.researchgate.net/profile/Lin_Qi12
Junyu Dong	full professor	Image processing, machine learning, computer vision	http://cvpr.ouc.edu.cn/people/dongjy.html
Xingnan Chen	master student	Machine learning	
Hui Yu	senior lecture	Computer vision, machine learning, computer graphics	http://www.port.ac.uk/school-of-creative-technologies/staff/hui-yu.html

*This form helps us to understand your paper better, **the form itself will not be published.**

*Title can be chosen from: master student, Phd candidate, assistant professor, lecture, senior lecture, associate professor, full professor